

# Blade Fault Diagnosis Based on Hybrid Physics and Domain Adaptation: A Case Study of Variable-Speed Marine Current Turbines

Tao Xie, Zhihuan Hu, Tianzhen Wang, Weidong Zhang, *Senior Member IEEE*, Hongtian Chen

**Abstract**—As a machine learning approach, domain adaptation methods are widely applied in cross-scenario fault diagnosis. However, the target domain may need more annotated data, posing challenges to the performance of domain adaptation methods. This paper proposes a fault diagnosis method based on hybrid physics and domain adaptation (HPDA) with its application to marine current turbines (MCTs) scenarios. Specifically, this method first establishes a rotational feature alignment model based on physical variables. Then, it aligns the feature of the target domain data with physical parameters. Finally, an augmented domain adversarial model is trained using pre-alignment samples. Data from MCT prototypes are collected to validate the effectiveness of the proposed method. Experimental results demonstrate the proposed method's superior stability and data transferability compared with the state-of-the-art.

**Index Terms**—Marine current turbines (MCTs), fault diagnosis, domain adaptation, synthetic data, physical feature.

## I. INTRODUCTION

**B**IOFOULING, caused by the accumulation of organisms and debris on the surfaces of marine current turbines (MCTs), has a significant impact on safety and stability [1]. Ocean currents represent a sustainable and renewable energy resource. The constant ocean tides and currents offer the potential for a continuous and reliable energy supply. Utilizing ocean currents can play a significant role in reducing traditional energy sources [2-3]. MCTs can be shared with other ocean infrastructure (e.g., ocean communication cables and observation equipment), reducing construction and maintenance costs. However, marine life attachment and bio-corrosion are common problems for MCT blades [4], where marine life (e.g., algae, shellfish, and barnacles) grow and attach to equipment surfaces, increasing hydrodynamic losses and potentially causing equipment damage [5-6]. Currently, the installation and deployment of MCTs are far less mature

than wind turbines (WTs) of the same construction. Therefore, more available fault samples must be available, which limits fault diagnosis methods [7-9]. As an underwater device, the deployment of vibration and image signals is very formidable, which limits the available data sources for MCTs [10-11]. Hence, this paper selects a current signal of MCTs for non-invasive online fault diagnosis.

Aiming at the problem of the unbalanced sample, several domain-adaptation (DA) techniques are used to generate discriminative and task-relevant features for domain adaptation [22]. Wang et al. [12] introduced domain discriminator entropy or uncertainty to select transferable local regions, albeit without proactive alignment with the image classification task. Wen et al. [13] focused on transferring primitive local feature patterns, which provide a fine-grained adaptation. Yu et al. [14] proposed a comprehensive rolling bearing fault diagnosis framework, incorporating domain adaptation and preferred feature selection. However, the feature extraction network limits the approach using parameter and model transfer cannot handle tasks involving significant distributional differences. Yu et al. [15] combined signal decomposition with domain adversarial adaptation for bearing fault diagnosis. Long et al. [16] developed a deep adaptation neural network (DANN) utilizing multi-kernel maximum mean discrepancy in all fully connected layers to learn transferable features across domains. Kuang et al. [17] presented an innovative adversarial transfer learning framework to address cross-domain fault diagnosis with imbalanced data. Guo et al. [18] introduced a novel DA network merging generative adversarial network technologies, demonstrating superior performance on transfer tasks across multiple datasets. To this end, distance-based domain adaptive methods suffer from decreased performance when the amount of target domain data in the training phase is restricted, as a common scenario in industrial power generation applications [19]. DA-based methods have shown great potential for fault diagnosis tasks. However, there still exist some drawbacks:

- 1) A case of significant differences in data distribution over variable operating conditions, which can lead to the performance degradation of the domain adaptive approach;
- 2) Since domain-adaptive methods must select or learn feature representations related to the target domain, the selection of feature representations with better generalization capabilities will have a significant impact on the

This work was supported in part by the National Natural Science Foundation of China under Grant 62303305, 62303308, U2141234, in part by Shanghai Pujang Program under Grant 23PJ1404700, in part by the National Key R and D Program of China under Grant 2022ZD0119900, in part by Shanghai Science and Technology program under Grant 22015810300, and in part by Hainan Province Science and Technology Special Fund under Grant ZDYF2021GXJS041.

T. Xie, Z. Hu, W. Zhang and H. Chen are with the Department of Automation, Shanghai Jiaotong University, Shanghai 200240, China; T. Wang is with Shanghai Maritime University, Shanghai, 201306, China; (e-mail: xietao0906@sjtu.edu.cn; scarlet@sjtu.edu.cn; tzwang@shmtu.edu.cn; wdzhang@sjtu.edu.cn; hongtian.chen@sjtu.edu.cn)

ability in migrating data.

The exploration for domain-enriched adaptive networks, enhanced by incorporating pre-existing physical priors, has captivated researchers for decades. Chen et al. [20] proposed an individual data sample enhanced method by considering the global data distribution. Mao et al. [21] employed domain-adversarial adaptive methods and introduced an incidence matrix to capture the inherent similarity structure among multiple fault types. In [22], an adaptive fault attention residual network was proposed for bearing diagnosis in circulating water pumps. The adaptive fault attention mechanism generated features strongly correlated with fault characteristics, ensuring meaningful knowledge transfer. Wen et al. [23] studied fault diagnosis dynamics centered around bearings, employing CNN training with an automatic learning rate scheduler. Yang et al. [24] introduced a deep transfer learning architecture for effective fault diagnosis of bogies under variable operating conditions, even without fault labels. To enhance domain adaptation capabilities, a deep joint distribution alignment was proposed to simultaneously reduce the discrepancy in marginal and conditional distributions between two domains [25]. Ye et al. [26] proposed an innovative fault diagnosis method for industrial robot joint bearings under varying working conditions. Wang et al. [27] presented a novel bearing fault diagnosis framework to learn effective models from unlabeled genuine bearing data. Notably, [27] demonstrated the generation of synthetic faults through expert knowledge and robust domain adaptation against data imbalance. Inspired by [27], Lu et al. [28] presented a novel fault diagnosis method based on spectrum alignment and deep transfer convolution neural network, where a data augmentation module is designed to extract fault features from the unbalanced bearing data. However, these methods need a physical interpretation of feature alignment to recognize the significance and flexibility of variable parameters in physical models during the domain adaptation process.

To address the aforementioned issues, this paper proposes an augmented domain adaptive fault diagnosis approach (HPDA) by incorporating the physical characteristics of machinery. The physical parameters of the diagnosed object are first considered to align the multi-domain features of the source and target domains. The multi-domain features are finely aligned by rotational sampling. Finally, the fault diagnosis of the target domain is accomplished by designing domain discriminators and classifiers. The main contributions are given as follows:

- 1) An augmented domain adaptive fault diagnosis network is developed to enhance fault diagnosis rates compared with existing methods. By incorporating the physical characteristics of the machinery, the network achieves improved diagnostic performance and exhibits significant application potential;
- 2) This innovative approach reduces local equipment upgrade costs and computational expenses while addressing the practical requirements of MCTs. Furthermore, the proposed method effectively addresses the issue of weakened features caused by variable marine currents;
- 3) Through the process of rotational alignment, the classi-

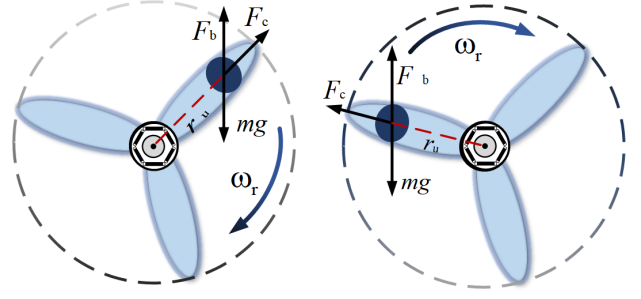


Fig. 1. The concept of blade biofouling cases.

fied network mitigates the impact of varying marine current (or operating conditions), increasing fault diagnosis accuracy. The effectiveness of the HPDA is demonstrated through two case studies, providing empirical validation of its capabilities.

The rest of this study is organized as follows. The basic knowledge is introduced in Section II, whose purpose is to expound on several preliminaries. Section III details the proposed HPDA, wherein the theoretical analysis and implementation procedures are presented. Section IV illustrates the effectiveness of the proposed fault diagnosis method via two applications to a practical MCT prototype and bearing beach. Section V concludes this study.

## II. PRELIMINARIES AND MOTIVATIONS

### A. Physical Paradigm and Fault Definitions

The biofouling of MCTs can be equivalent to attaching a virtual mass to the rotational blade. As shown in Fig. 1, the mass rotates periodically with the MCTs blade at the angular velocity  $\omega_r$ . The buoyancy  $F_b$  and the gravity of mass generate an additional torque [29]:

$$T_{im} = (mg - F_b) * r_u \sin(\omega_r t + \varphi), \quad (1)$$

where  $m$  denotes the quality of mass;  $g$  denotes the gravitational acceleration;  $r_u$  denotes the distance between the mass and the center of the shaft;  $\varphi$  denotes the initial phase.

The angular velocity  $\omega_n$  under the blade biofouling state is:

$$\omega_n = -\frac{(mg - F_b)r_u \cos(\omega_r t + \varphi)}{J\omega_r} + \omega_r = \Delta\omega_r + \omega_r, \quad (2)$$

where  $\Delta\omega_r$  denotes the change in turbine angular velocity with blade biofouling. It equals to zero when the MCTs working under healthy states. The stator current of MCTs with blade fouling can be expressed as follows:

$$i_s(t) = A_t \sin(p(\omega_r + \Delta\omega_r)t + \varphi), \quad (3)$$

where  $A_t$  denotes the amplitude of the stator current;  $p$  denotes the number of pole pairs. The instantaneous frequency of the stator current can be expressed as follows:

$$f(t) = pf_{im} - \frac{b}{2\pi} \cos(2\pi f_{im}t + \varphi), \quad (4)$$

where  $b$  denotes the coefficient of blade biofouling;  $f_{im}$  is the physical fault frequency. The physical frequency can be considered as the characteristic variable of data from MCTs, which will support domain adaptation.

### B. Domain Adaptation

The domain adaptation problem concerning fault diagnosis for MCTs is defined as follows:

*Definition 1.* The source domain, denoted as  $\mathcal{D}_s = \{(x_i^s, y_i^s)\}_{i=1}^{n_s}$ , consists of  $n_s$  MCTs source samples with corresponding labels  $y_i^s$  drawn from the distribution  $\mathcal{P}_s$ . The source samples pertain to  $|\mathcal{C}_s|$  distinct classes, where  $\mathcal{C}_s$  denotes the label space associated with the source domain.

*Definition 2.* Additionally, the target domain is represented as  $\mathcal{D}_t = \{x_i^t\}_{i=1}^{n_t}$ , encompassing  $n_t$  unlabeled MCT samples  $x_i^t$  drawn from the distribution  $\mathcal{P}_t$ . The target samples belong to  $|\mathcal{C}_t|$  classes, with  $\mathcal{C}_t$  signifying the label space of the target domain.

*Definition 3.* Assuming that the data in the source and target domains are sufficient and follow different distributions, denoted by  $\mathcal{P}_s \neq \mathcal{P}_t$ . The source and target domains share an identical label space, represented by  $\mathcal{C}_s = \mathcal{C}_t$ . Furthermore, the sample distribution is balanced across all source and target domain categories.

The primary objective of this study is to design a function that could be achieved via a neural network, denoted as  $f^*$ , which effectively minimizes the discrepancy between the marginal and conditional distributions. This process facilitates the acquisition of domain-invariant features, ensuring that  $y_i^s = f^*(x_i^s)$  and  $y_i^t = f^*(x_i^t)$ . Remarkably, the universality of  $f^*$  across the domains is guaranteed by the shift assumption.

### C. Motivations

As mentioned target domain  $\mathcal{D}_t$  in *Definition 2*, selecting key alignment features with the source domain data is essential. Because of different flow velocities (rotational conditions), the variable distributional feature will cause the trained model to overfitting. The data features are varying under different rotational conditions. If the rotational drift can be estimated and quantified, and the data feature corresponding to different domains can be aligned by the compensation, allowing the source and target domains to share the same diagnosis model. However, aligning features that lack physical meaning will not serve the purpose of effective domain invariance. Based on this observation, physical parameters such as mechanical rotation and sampling frequency can provide a good set of aligned features to domain adaptive adversarial training.

## III. FAULT DIAGNOSIS FRAMEWORK

### A. Designs of Rotational Alignment

Due to the diverse effects of varying flow rates on the raw signals acquired from the MCT, the data distribution exhibits heterogeneity. Consequently, the existing deep learning-based fault diagnosis models exhibit relatively weak domain invariance and generalization capabilities. Therefore, it is imperative

to devise an appropriate feature alignment and scaling transformation method to enhance the representativeness of input features within domain adversarial networks. Specifically, the feature alignment between the source and target domains are achieved by estimating physical parameters. Subsequently, a periodic second-order resampling of features is conducted to align the stable fault characteristics. Under different fault scenarios, the phase current encompasses distinct fault-related information, wherein rotational alignment and feature sampling play key roles in building domain adversarial models.

#### Step1: Specific-prior knowledge gaining

Speeds and frequencies, as a priori of MCTs, need to be acquired first. Hilbert transform (HT) is an useful technique for extracting time-frequency features. HT can be represented as follows:

$$H(u)_{(s,t)} = \frac{1}{\pi} p.v. \int_{-\infty}^{+\infty} \frac{u_{(s,t)}(\tau)}{t - \tau} d\tau, \quad (5)$$

where  $p.v.$  stands for the Cauchy principal value, which is the integral value of the flawed integral;  $u_{(s,t)}$  is the original signal. Then, the instantaneous rotational frequency can be founded by the phase derivative as follows:

$$\omega_{(s,t)}(t) = \frac{\text{darctg} \frac{Hu_{(s,t)}}{u_{(s,t)}}}{dt}, \quad (6)$$

where  $\text{arctg}(-)$  is the derivative function.

#### Step2: Compensation alignment

When the instantaneous frequency is captured, the real-time rotational velocity of MCTs can be accurately characterized. Therefore, the data characteristics at different flow rates can be aligned utilizing compensation, expressed as follows:

$$u(f) = \int_{-\infty}^{\infty} u(t) \exp(-2\pi j(f_r t) - \omega^\perp j) dt. \quad (7)$$

*Remark 1.* The compensation parameter  $\omega^\perp$ , together with the corresponding objective alignment feature given in (7), play an essential role in the domain adaptation for fault diagnosis. It benefits from the physical variables that can transform domain-variant features into common features.

The compensation parameter is defined as the frequency difference between the source and target domains, which is given as

$$\omega^\perp = \hat{\omega}_s - \hat{\omega}_t. \quad (8)$$

*Remark 2.* By using the frequencies as the domain compensation, the compensation alignment transformation in (7) can achieve the purpose of normalized data from the source and target domains. The difference to be compensated is the portion of the rotation frequency  $\hat{\omega}_t$  in the source domain that exceeds the target domain  $\hat{\omega}_s$ , it will be compensated for in the target space, leaving the completed domain invariant. This rotation compensation applies equally to any sample period.

Additionally, since the transient frequency is an essential feature of MCT blade faults, the proposed HPDA approach uses the diagnosis-relevant features  $\hat{\omega}$  for domain shift alignment, which improves fault diagnosis accuracy.

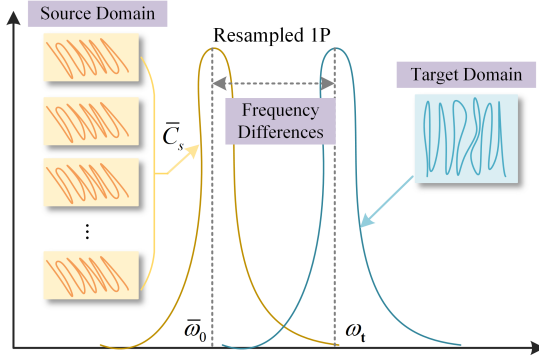


Fig. 2. The procedure of telescoping modulus.

### Step3: Frequency proportional normalization

Although the fault characteristics can be better displayed in the frequency domain, the spectrum leakage still exists, and this advantage will be transformed into a disadvantage, thus affecting the fault diagnosis result. The processing of the time domain signal need to be more in-depth as compared to the frequency domain signal. Base on this observation, the aligned time domain signal need to be obtained though inverse transformation and further re-sampled to acquire a concentrated feature. Fourier inversions can transfer the aligned frequency domain data  $u(f)$  into a new source (target) domain signal, which can be given as

$$u^*(t) = \mathcal{F}^{-1}[u(\omega)]. \quad (9)$$

When the sampling frequency is proportional to the instantaneous signal, the sampled instantaneous signal is a fixed value. It can be calculated though Fourier transform. Therefore, the fault characteristic signal will change from non-stationary to stable, which can be expressed as

$$F_{\text{cons}} = \int_{-\infty}^{\infty} u^*(t) \exp(-2\pi j\omega) dt \quad s.t. f_s = f_s(t), \quad (10)$$

where  $f_s$  donates the variable sampling frequency. The instantaneous signal is expected to be stable after resampling. To satisfy with (10), the rotation frequency of MCTs in (6) can be discretized to the known instantaneous rotation frequency, which is a fixed value. It can be deduced as follows:

$$F_{\text{cons}} = \frac{1}{N_f} \sum_{n_f=0}^{N_f} f_g[n_f], \quad (11)$$

where  $n_f = 1, 2, \dots, N_f$  is the number of samples. Defining the initial value as 1, the step size is solved in each interpolation according to the variable sampling accumulation method. The following equation updates the sequence of subsequent variable steps

$$S_1[n_f + 1] = S_1[n_f] + \frac{F_{\text{cons}}}{f_g[n_f]}. \quad (12)$$

The computed orthogonal frequency sequence can be used to interpolate the new signal. Furthermore, the rotational frequency signal is updated by the new signal with HT.

### Algorithm 1 Fault diagnosis based on HPDA.

---

```

1: Input Dataset  $\mathcal{D}^s = \{\mathbf{x}_i^s, y_i^s\}_{i=1}^{n_s}, \mathcal{D}^t = \{\mathbf{x}_i^t\}_{i=1}^{n_t}$ , batch size, max epoch.
2: Output MCT fault categories  $\Xi = \{H, \Xi_1 - \Xi_n\}$ .
3: For  $epoch = 1, 2, \dots, maxepoch$  do
4:   For  $step = 1, 2, \dots, maxstep$  do
5:     Calculate source domain features  $g^s = G(\mathbf{x}^s)$ 
6:     Calculate target domain features  $g^t = G(\mathbf{x}^t)$ 
7:     Compensation alignment with  $\omega_{\perp}$  in (8)
8:     Calculate the domain prediction  $y^d = D(\mathbf{x}^{t,s})$ 
9:     Calculate the target prediction  $y^t = C(\mathbf{x}^t)$ 
10:    Calculate loss from discriminator and classify
11:    Calculate the gradient and update parameters
12:   end For
13: end For
14: Obtain target optimization categories
15: Return  $\Xi$ 
16: End of Pseudo-Code

```

---

### B. Augmented Domain Adaptation

The following will construct a domain adversarial network by combining pre-aligned feature sets of the source and target domains. The network will be trained against supervised source domain data by adjusting the rotational alignment parameters and domain discriminator parameters. Therefore, the target domain fault class can be identified using a classifier. The task of domain-invariant can be re-formulated as follows.

1) The source domain data with rotational alignment samples are given as

$$\mathcal{D}_s = \{(x_s^1, y_s^1), \dots, (x_s^n, y_s^n)\}, \quad y_s^i \in Y. \quad (13)$$

2) Base on Definition 2, the unlabeled real data from the target domain are given as

$$\mathcal{D}_t = \{x_t^1, \dots, x_t^m\}. \quad (14)$$

3) A block issue for the rotational alignment: In MCT scenarios, different flow rates and external environments will inspire the data to present multiple batches, which will test the data length and frequency selection for rotational alignment. Once the appropriate data length is not selected at a particular flow rate, it will affect the quality of the alignment of the source and target domain features, weakening the domain adaptive network and generating misdiagnosis of MCT faults.

To this end, given an expansion extractor  $\varsigma$  parameterized by  $\theta_{\varsigma}$ , a discriminator  $g$  parameterized by  $\theta_g$ , a generator  $d$  parameterized by  $\theta_d$ , the proposed method is essentially solving the following equation

$$\mathcal{L}(\theta_{\mathcal{F}}, \theta_c, \theta_h) = \mathcal{L}_{\text{clf}}(c(\mathcal{F}(x))) - \lambda_d \mathcal{L}_d(h(\mathcal{F}(x))). \quad (15)$$

It can reversely adjust the expansion coefficient in the decomposition procedure by minimizing and obtaining the optimal solution as

$$\{\hat{\theta}_c, \hat{\theta}_{\mathcal{F}}\} = \arg \min_{\theta_c, \theta_{\mathcal{F}}} \chi(\theta_g, \theta_{\mathcal{F}}, \hat{\theta}_d). \quad (16)$$



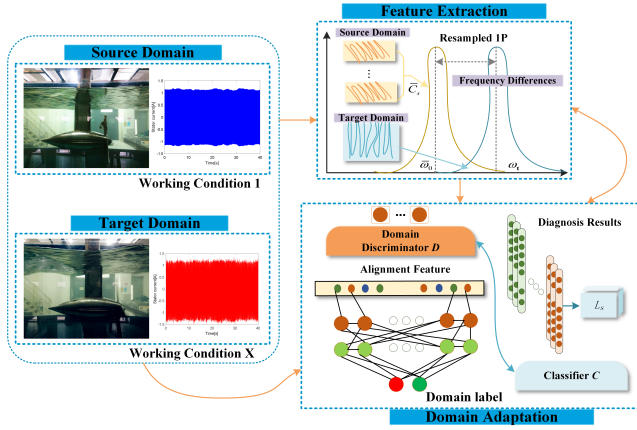


Fig. 3. The procedure of the HPDA approach.

*Remark 3.* The optimized hyperparameters  $\theta_{\mathcal{F}}$  can be employed to update new synthetic sample matrices  $U_{\mathcal{F}}$ . This optimization process in (16) enables reverse-optimize and adjusts the parameter in sample expansion models. As a result, a closed loop is formed between the physical feature and the discrimination of the original sample, enabling interactive linkage and cross-fusion of the physical knowledge and data features.

### C. Framework Structures

In order to transfer the fault-relevant feature from the source to the target domain, which can be split into three parts: feature alignment, domain adaptation, and fault diagnosis, as illustrated in Fig. 3. The data from both the source and target domains are projected into the frequency space for aligning during the feature extraction, and then filters are used to identify fault-relevant features. Domain adversarial models are used in the domain adaptation to reduce feature discrepancies in the marginal and conditional distributions. The classifier is trained with source data supervision for fault diagnosis. Three optimization goals are listed below. a) Reduce the  $\theta_c$  by using data from the source domain. b) Maximize the  $\theta_{\mathcal{F}}$  by using data from the source and target domains. c) The  $\theta_d$  with the source and target domains should be minimized.

## IV. CASE STUDIES

This section validates the proposed method by using the SMUD-600 prototype dataset and the rotor-bearing beach dataset. All experiments are conducted in the Win10 environment using Pycharm 3.1. The transfer tasks are defined as from source domains to target domains.

### A. Case 1: SMUD-600

#### 1) Experimental setup and dataset descriptions

An experimental framework is established to facilitate rigorous inquiry, encompassing a 0.23 kW direct-drive permanent magnet synchronous generator (PMSG), as illustrated in Fig. 4. The experimental platform includes several components: turbines, a PMSG, a comprehensive data acquisition system,

TABLE I  
SPECIFICATIONS OF THE MCT SYSTEM PARAMETERS

PMSG	Parameters	Turbine	Parameters
Pole-pair	8	Airfoil	NACA 0808
Flux	0.18 Wb	Pitch Angle	12.6°
Inductance	11.8 mH	Chord Length	0.2-0.3 m
Resistance	3.3 Ω	Blade Diameter	0.6 m

and an intricately designed state monitoring infrastructure. The detailed parameters can be referenced from Table I. The PMSG prototype adopting a meter stick design characterized by 8 pole pairs. The vertical shaft of the generator was positioned at an elevation of 0.6 meters above the water surface.

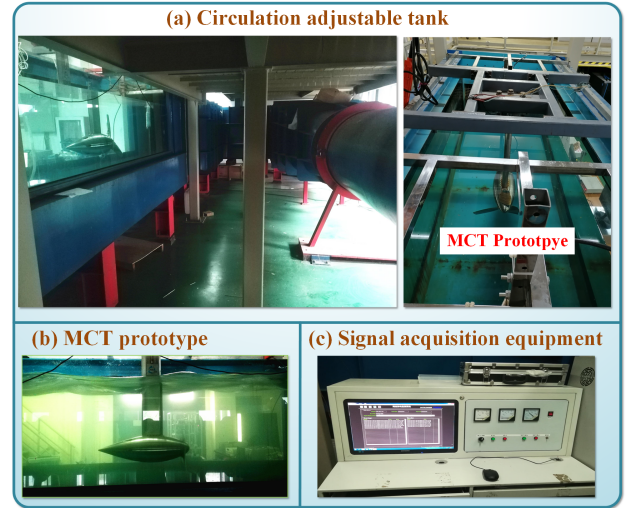


Fig. 4. The MCTs prototype in variable water-flow.

In this study, a string replicates the entanglement encountered in submarine environments. This case study is conducted by manipulating the string mass, which is adjusted to imitate the biofouling of blades. Since attachments cannot increase continuously, maintenance shutdowns are performed within a certain threshold [30]. Five fault cases have been designed as follows based on the upper limit of the attachment effect on the blades.

- 1) Healthy  $b_1$ : No attached string.
- 2) Biofouling1  $b_2$ : Fault degree parameter  $s = 0.05$ , a piece of the string is attached onto the blade (50g).
- 3) Biofouling2  $b_3$ : Fault degree parameter  $s = 0.10$ , a piece of the string is attached onto the blade (101g).
- 4) Biofouling3  $b_4$ : Fault degree parameter  $s = 0.15$ , a piece of the string is attached onto the blade (150g).
- 5) Biofouling4  $b_5$ : Fault degree parameter  $s = 0.20$ , a piece of the string is attached onto the blade (202g).

The water flow regulator of the experimental platform generates variable operating conditions. The stator current signal under varying operating conditions is collected when the variable flow velocity is changed from 0.9m/s to 1.4m/s. In each flow velocity interval, the wave-pressing plate and the wave-making motor provide a natural ocean current environment to simulate the seawater expansion effect and the random

surge. Hence, the flow velocity changes up and down at an average flow velocity. The stator current signal of SMUD-600 is collected under four operating conditions (flow rates).

- 1) Task A  $c_1$ : Water flow speed  $c = 0.9\text{m/s}$ .
- 2) Task B  $c_2$ : Water flow speed  $c = 1.1\text{m/s}$ .
- 3) Task C  $c_3$ : Water flow speed  $c = 1.2\text{m/s}$ .
- 4) Task D  $c_4$ : Water flow speed  $c = 1.3\text{m/s}$ .

Fig. 5 illustrates the frequency spectrum of the current signal under four operation conditions. It can be seen that the frequency of target samples fails to align due to the variable current speed, and the scattered frequency also makes the feature extraction difficult.

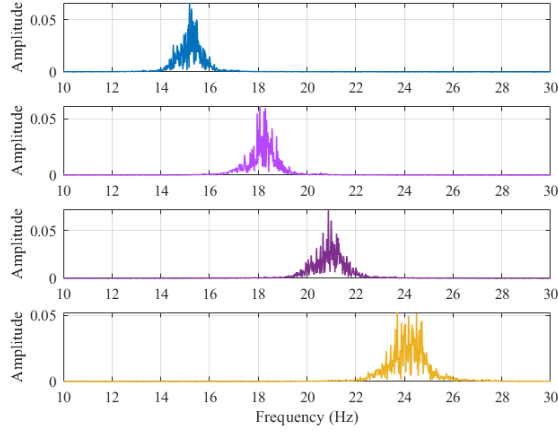


Fig. 5. The frequency analysis of the current signal under different cases.

## 2) Implementation details

In this study, due to the SMUD-600 dataset having varying distribution under four operating conditions, the transfer tasks can be defined as  $A/B \rightarrow C$ ,  $A/C \rightarrow B$ ,  $B/C \rightarrow A$ ,  $A/B \rightarrow D$ , and  $A/C \rightarrow D$ . For instance, the transfer task  $A/B \rightarrow C$  indicates that a model trained on the source data collected under flow rates of  $0.9\text{m/s}$  or  $1.1\text{m/s}$  will transfer to the unlabeled target data collected under a flow rate of  $1.2\text{m/s}$ . The hyperparameters of all comparison methods are the same to ensure the fairness of comparisons. Specifically, CNN has two convolution layers with 8 and 16 convolution cores, respectively. The kernel length is 3. The weight attenuation coefficient of L2 regularization is 0.0001.

## 3) Approaches for comparison studies

To verify the effectiveness and superiority of the HPDA approach, this study conducts a comprehensive experiment involving five distinct approaches within the cross-domain diagnosis scenarios. These comparison methods are carefully selected to ensure similar network architectures and experimental configurations, thereby facilitating a fair and insightful evaluation of the HPDA's performance.

1) Without domain adaptation: A baseline convolutional residual network without domain adaptation is conducted for comparisons. Specifically, the proposed network model is trained by labeled source samples and directly used for data from the target domain.

2) DNCNN and DTCNN: In [27], two classifiers were introduced to the network structure, and the domain adaptation was achieved by maximizing the discrepancy between the two

TABLE II  
COMPARISONS WITH CLASSICAL METHODS

Cross Test	A/B $\rightarrow$ C	A/C $\rightarrow$ B	B/C $\rightarrow$ A	A/B $\rightarrow$ D	A/C $\rightarrow$ D	Average
CNN	78.78	76.54	65.13	71.24	75.24	71.33
DNCNN	76.33	77.48	80.20	81.31	77.32	78.41
DTCNN	81.78	83.21	80.91	81.34	85.87	81.65
AFARN	88.90	96.11	90.23	89.10	87.35	91.43
DANN	88.78	86.94	85.44	83.74	85.10	81.90
HPDA	94.78	96.10	95.36	93.34	97.20	93.96

classifier's outputs. This idea was used in cross-domain fault diagnosis [28].

3) AFARN: In [22], a particular gradient reversal layer was introduced to implement adversarial learning of the domain classifier to achieve domain-invariant knowledge.

4) DANN: The maximum mean discrepancy has been widely used in the existing literature as a statistical moment-matching approach. Thus, a fundamental discrepancy loss-based approach is established for comparisons.

The evaluation metric for the target diagnosis accuracy is the diagnosis performance, which is specified as  $\text{accuracy} = \sum_{i=1}^N \psi(y_i^t, \hat{y}_i^t) / N$ .

## 4) Diagnosis results and ablation tests

Fig. 6 illustrates the frequency spectrum of the current signal under four operation conditions after the HPDA approach. It can be seen that the frequency samples from the different tasks are aligned well. The comprehensive comparison analysis with state-of-the-art methods has also verified the superiority of the HPDA approach. In contrast, the recognition accuracy of CNN with the worst performance is only 71.33% at the lowest. The diagnostic accuracy from different transfer tasks are listed in TABLE II. The same conclusion can be found. The proposed method has significant advantages over other methods.

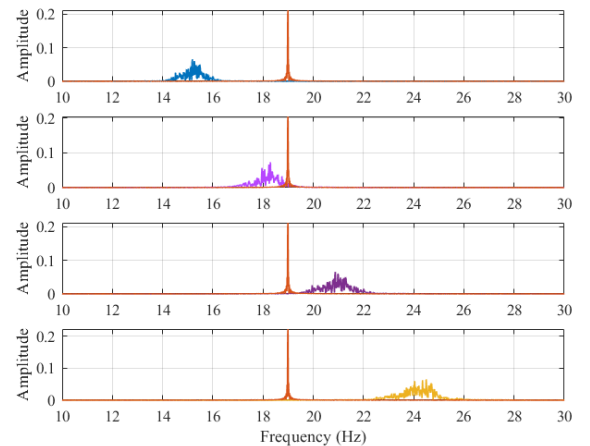


Fig. 6. The frequency analysis of the current signal after alignments.

In order to further validate the effectiveness of the proposed HPDA approach, ADA is implemented for the ablation test. Different labels  $\mathcal{L}$  of MCT faults are used to compare and prove the superiority of the proposed methods ( $\mathcal{L} = 0, 1, 2, 3, 4$ ), and the fault diagnosis accuracy is shown in Fig.

7. It can be found that the diagnostic accuracy under the proposed method is higher than ADA.

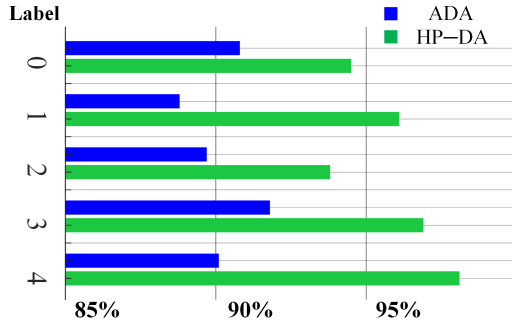


Fig. 7. The diagnosis results between the HPDA and ADA.

### B. Case 2: Rotor-bearing test bench dataset

#### 1) Experimental Setup and Dataset Descriptions

A bearing dataset is obtained from a rotor-bearing test bench to further quantify the bearing fault diagnosis results, as shown in Fig 8. In order to apply the HPDA approach, three fault cases are designed as follows based on the upper limit of the attachment effect on bearings.

- 1) Healthy  $I_1$ : No attached mass.
- 2) Imbalance1  $I_2$ : Fault degree parameter  $i = 0.02$ , a piece of the mass is attached to the bearing (20g).
- 3) Imbalance2  $I_3$ : Fault degree parameter  $i = 0.04$ , a piece of the mass is attached to the bearing (40g).
- 4) Imbalance3  $I_4$ : Fault degree parameter  $i = 0.06$ , a piece of the mass is attached to the bearing (60g).

Each class consists of 2,000 samples representing a vibration signal containing 1024 data points.

#### 2) Approaches for Comparison Studies

To eliminate the random errors, the average of the last ten training results are used as the final accuracy, with the training and test samples being randomly selected in each iteration. A CNN classification method with consistent hyperparameters is employed to evaluate the effectiveness of the physics-informed multifractal features. Similar to SMU600 dataset, the distribution of the investigated dataset varies among four operating (load) conditions, which are defined as A, B, C, and D. Therefore, the transfer tasks can be defined as  $A/B \rightarrow C$ ,  $A/C \rightarrow B$ ,  $B/C \rightarrow A$ ,  $A/B \rightarrow D$ , and  $A/C \rightarrow D$ .

#### 3) Diagnosis Results

The average accuracy across these experiments is presented in TABLE III. Notably, the proposed HPDA-CNN method demonstrates favorable performance when applied to the bearing fault dataset.

### C. Discussions

Aiming at the imbalance problem of underwater generations, a method to improve fault diagnosis performance under variable marine conditions is proposed. The following insights and findings can be inferred as follows.

- 1) The HPDA approach outperforms the existing methods in diagnosis performance: The two case studies reflect

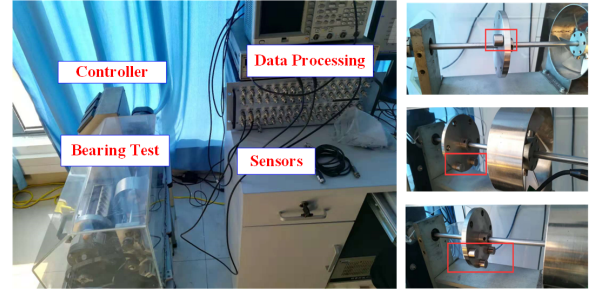


Fig. 8. The platform of rotor-bearing test bench.

TABLE III  
COMPARISONS WITH CLASSICAL METHODS

Cross Test	A/B $\rightarrow$ C	A/C $\rightarrow$ B	B/C $\rightarrow$ A	A/B $\rightarrow$ D	A/C $\rightarrow$ D	Average
CNN	78.78	76.54	65.13	71.24	75.24	71.33
DNCNN	76.33	77.48	80.20	81.31	77.32	78.41
DTCNN	81.78	83.21	80.91	81.34	85.87	81.65
AFARN	88.90	96.11	90.23	89.10	87.35	91.43
DANN	88.78	86.94	85.44	83.74	85.10	81.90
HPDA	94.78	96.10	95.36	93.34	97.20	93.96

a unified situation of fusing physical knowledge, i.e., synergistic use of physical knowledge contributes to the diagnosis process. In addition, the issue of diagnostic capability in a realistic scenario is considered. From the experimental results, the proposed HPDA method outperforms the existing methods in all cases, mainly regarding accuracy;

- 2) Demodulation methods: Since HT demodulates the current signal of MCT as a pre-processing, it will inevitably cause the end effect of the signal. Therefore, the optimization of the signal demodulation algorithm can be used as the future research;
- 3) Feasibility of other various applications: The mechanistic model may change due to environmental factors, and only the most accurate physical information can drive the feature to generate fault-relevant information. Since various application backgrounds generate different signals, more evaluation factors may need to be selected as the constraint of the objective function.

### V. CONCLUSIONS

This paper proposed a novel HPDA method for MCT blade fault diagnosis. The extraction capability of signal frequency features is enhanced by introducing the fault physical frequency into the domain adaptation technology, ultimately improving the fault diagnosis accuracy. Besides, the MCT prototype test platform was established for data collection and method validation. In both cases, the experimental results show that HPDA has better feature alignment capability and diagnostic performance than the traditional method. It is a new and general fault diagnosis scheme with good prospects in engineering applications. However, the proposed approach still needs to be improved as it requires deployed MCT fault data, which is inconsistent with MCT applications: the known blade



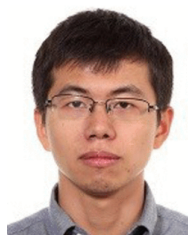
fault datasets are hardly achieved due to harsh waterproof requirements and hostile environments.

## REFERENCES

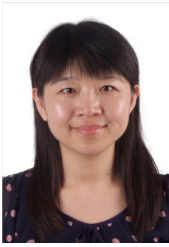
- [1] B. Barnier, A. Domina, S. Gulev, J. M. Molines, T. Maitre, T. Penduff, P. Colombo, "Modelling the impact of flow-driven turbine power plants on great wind-driven ocean currents and the assessment of their energy potential," *Nature Energy*, vol. 5, no. 3, pp. 240-249, 2020.
- [2] A. Farkas, N. Degiuli, I. Martić, M. Barbarić, and Z. Guzović, "The impact of biofilm on marine current turbine performance," *Renewable Energy*, vol. 190, pp. 584-595, 2022.
- [3] B. Pan, L. Wang, Z. Zhang, Z. Li, and Z. Yang, "Whisk-inspired motion converter for ocean wave energy harvesting," *IEEE/ASME Transactions on Mechatronics*, vol. 27, no. 3, pp. 1808-1811, June 2022.
- [4] M. Cobb et al., "Iterative learning-based path optimization with application to marine hydrokinetic energy systems," *IEEE Transactions on Control Systems Technology*, vol. 30, no. 2, pp. 639-653, 2022.
- [5] W. Tian, X. Ni, Z. Mao, and T. Zhang, "Influence of surface waves on the hydrodynamic performance of a horizontal axis ocean current turbine," *Renewable Energy*, vol. 158, pp. 37-48, 2020.
- [6] B. Freeman, Y. Tang, Y. Huang, and J. VanZwieten, "Physics-informed turbulence intensity infusion: A new hybrid approach for marine current turbine rotor blade fault detection," *Ocean Engineering*, vol. 254, 111299, 2022.
- [7] Q. Yang, G. Liu, Y. Bao and Q. Chen, "Fault detection of wind turbine generator bearing using attention-based neural networks and voting-based strategy," *IEEE/ASME Transactions on Mechatronics*, vol. 27, no. 5, pp. 3008-3018, 2022.
- [8] Z. Su, X. Zhang, G. Wang, S. Wang, M. Luo and X. Wang, "The semisupervised weighted centroid prototype network for fault diagnosis of wind turbine gearbox," *IEEE/ASME Transactions on Mechatronics*, 2023.
- [9] Y. Gao, X. Liu and J. Xiang, "Fault detection in gears using fault samples enlarged by a combination of numerical simulation and a generative adversarial network," *IEEE/ASME Transactions on Mechatronics*, vol. 27, no. 5, pp. 3798-3805, 2022.
- [10] H. Chen, L. Li, C. Shang and B. Huang, "Fault detection for nonlinear dynamic systems with consideration of modeling errors: A data-driven approach," *IEEE Transactions on Cybernetics*, vol. 53, no. 7, pp. 4259-4269, 2023.
- [11] H. Chen, H. Luo, B. Huang, B. Jiang and O. Kaynak, "Transfer Learning-motivated intelligent fault diagnosis designs: A survey, insights, and perspectives," *IEEE Transactions on Neural Networks and Learning Systems*, doi: 10.1109/TNNLS.2023.3290974.
- [12] Z. Wang et al., "Differential treatment for stuff and things: A simple unsupervised domain adaptation method for semantic segmentation," in *Proc. IEEE Comput. Soc. Conf. Comput. Vis. Pattern Recognit.*, 2020, pp. 12635-12644.
- [13] J. Wen, J. Yuan, Q. Zheng, R. Liu, Z. Gong, and N. Zheng, "Hierarchical domain adaptation with local feature patterns," *Pattern Recognit.*, vol. 124, 2022, Art. no. 108445.
- [14] X. Yu et al., "Rolling bearing fault diagnosis based on domain adaptation and preferred feature selection under variable working conditions," *Shock Vibrat.*, vol. 2021, pp. 1-27, Jan. 2021.
- [15] X. Yu, B. Xia, S. Yang, H. Yin, Y. Wang, and X. Liu, "A deep domain-adversarial transfer fault diagnosis method for rolling bearing based on ensemble empirical mode decomposition," *J. Sensors*, vol. 2022, pp. 1-18, May 2022.
- [16] M. Long, Y. Cao, J. Wang, and M. I. Jordan, "Learning transferable features with deep adaptation networks," in *Proc. Int. Conf. Mach. Learn.*, 2015, pp. 97-105.
- [17] J. Kuang, G. Xu, T. Tao, and Q. Wu, "Class-imbalance adversarial transfer learning network for cross-domain fault diagnosis with imbalanced data," *IEEE Transactions on Instrumentation and Measurement*, vol. 71, pp. 1-11, 2022.
- [18] L. Guo, Y. Lei, S. Xing, T. Yan, and N. Li, "Deep convolutional transfer learning network: A new method for intelligent fault diagnosis of machines with unlabeled data," *IEEE Transactions on Industrial Electronics*, vol. 66, no. 9, pp. 7316-7325, Sep. 2019.
- [19] H. Chen, H. Luo, B. Huang, B. Jiang and O. Kaynak, "Transfer learning-motivated intelligent fault diagnosis designs: a survey, insights, and perspectives," *IEEE Transactions on Neural Networks and Learning Systems*, doi: 10.1109/TNNLS.2023.3290974.
- [20] C. Chen, F. Shen, J. Xu, and R. Yan, "Domain adaptation-based transfer learning for gear fault diagnosis under varying working conditions," *IEEE Transactions on Instrumentation and Measurement*, vol. 70, pp. 1-10, 2021.
- [21] W. Mao, Y. Liu, L. Ding, A. Safian, and X. Liang, "A new structured domain adversarial neural network for transfer fault diagnosis of rolling bearings under different working conditions," *IEEE Transactions on Instrumentation and Measurement*, vol. 70, pp. 1-13, 2021.
- [22] W. Cheng et al., "AFARN: Domain adaptation for intelligent cross-domain bearing fault diagnosis in nuclear circulating water pump," *IEEE Transactions on Industrial Informatics*, vol. 19, no. 3, pp. 3229-3239, March 2023.
- [23] L. Wen, L. Gao, X. Li, and B. Zeng, "Convolutional neural network with automatic learning rate scheduler for fault classification," *IEEE Transactions on Instrumentation and Measurement*, vol. 70, 2021.
- [24] B. Yang, T. Wang, J. Xie, and J. Yang, "Deep adversarial hybrid domain-adaptation network for varying working conditions fault diagnosis of high-speed train bogie," in *IEEE Transactions on Instrumentation and Measurement*, vol. 72, pp. 1-10, 2023.
- [25] Y. Qin, Q. Qian, J. Luo, and H. Pu, "Deep joint distribution alignment: A novel enhanced-domain adaptation mechanism for fault transfer diagnosis," in *IEEE Transactions on Cybernetics*, vol. 53, no. 5, pp. 3128-3138, May 2023.
- [26] Z. Ye and J. Yu, "Deep negative correlation multisource domains adaptation network for machinery fault diagnosis under different working conditions," in *IEEE/ASME Transactions on Mechatronics*, vol. 27, no. 6, pp. 5914-5925, Dec. 2022.
- [27] Q. Wang, C. Taal, and O. Fink, "Integrating expert knowledge with domain adaptation for unsupervised fault diagnosis," in *IEEE Transactions on Instrumentation and Measurement*, vol. 71, pp. 1-12, 2022.
- [28] F. Lu, Q. Tong, Z. Feng, and Q. Wan, "Unbalanced bearing fault diagnosis under various speeds based on spectrum alignment and deep transfer convolution neural network," in *IEEE Transactions on Industrial Informatics*, vol. 19, no. 7, pp. 8295-8306, July 2023.
- [29] T. Xie, W. Zhang, Y. Zhang, Z. Ahmed, and Y. Tang, "Marine current turbine multi-fault diagnosis based on optimization resampled modulus feature and 1D-CNN," *IEEE Transactions on Instrumentation and Measurement*, 2023.
- [30] X. Gong and W. Qiao, "Current-based mechanical fault detection for direct-drive wind turbines via synchronous sampling and impulse detection," *IEEE Transactions on Industrial Electronics*, vol. 62, no. 3, pp. 1693-1702, March 2015.



**Tao Xie** (Member, IEEE) was born in China, in 1993. He received the Ph.D. degree in electrical engineering in 2022 from Shanghai Maritime University, Shanghai, China. From 2020 to 2021, He funded by the ISblue laboratory, France, as an Doctoral Mobile Fellow. He is currently a Postdoctoral Fellow with Shanghai Jiao Tong University, Shanghai, China. He was selected for the 2022 Shanghai Super Postdoctoral Incentive Program. He also received youth foundation from NSFC, in 2023. His research interests include control theory, machine learning theory, and their applications in power generation systems.



**Zhihuan Hu** received the B.Sc. degree in naval technology from Dalian University of Technology, Dalian, China, and the M.Sc. degree in ocean engineering from Shanghai Jiao Tong University, Shanghai, China, where he is currently working toward the Ph.D. degree in automation. His research interests include motion planning and control for autonomous surface vehicle.



**Tianzhen Wang** (Member, IEEE) was born in Qingdao, China, in 1978. She received the B.S. degree in industrial automation from the Shandong University of Technology, Shandong, China, in 2001, and the Ph.D. degree in power electronics and power drive from Shanghai Maritime University, Shanghai, China, in 2006. She is a Full Professor at Shanghai Maritime University and Research Affiliate and Doctoral Supervisor of the Institute de Recherche Dupuy de Lôme (IRDL). Her research interests include fault diagnosis, fault-tolerant control methods,

applications in inverters, wind power generators, and ocean current machines.



**Weidong Zhang** (Member, IEEE) received his BS, MS, and PhD degrees from Zhejiang University, China, in 1990, 1993, and 1996, respectively, and then worked as a Postdoctoral Fellow at Shanghai Jiaotong University. He joined Shanghai Jiaotong University in 1998 as an Associate Professor and has been a Full Professor since 1999. From 2003 to 2004 he worked at the University of Stuttgart, Germany, as an Alexander von Humboldt Fellow. From 2013 to 2017 he serviced as Deputy Dean of the Department of Automation. He is a recipient of National Science

Fund for Distinguished Young Scholars, China. He is currently Director of the Engineering Research Center of Marine Automation Shanghai Municipal Education Commission, China. His research interests include control theory, machine learning theory, and their applications in industry and autonomous systems. He is the author of more than 300 papers and 1 book, and has been recognized as an Elsevier most cited researcher.



**Hongtian Chen** (Member, IEEE) received his Ph.D. degree in College of Automation Engineering from Nanjing University of Aeronautics and Astronautics, China, in 2019. He was a Post-Doctoral Fellow at the University of Alberta, Canada, from 2019 to 2023.

Dr. Chen joined Shanghai Jiao Tong University, China in 2023 as an Associate Professor in the Department of Automation. His research interests include fault diagnosis and fault-tolerant control, data mining and analytics, machine learning, and cooperative control; and their applications in high-speed trains, new energy systems, industrial processes, and autonomous systems.

Dr. Chen was a recipient of the Grand Prize of Innovation Award of Ministry of Industry and Information Technology of the People's Republic of China in 2019, the Excellent Ph.D. Thesis Award of Jiangsu Province in 2020, the Excellent Doctoral Dissertation Award from Chinese Association of Automation (CAA) in 2020, and Marie Skłodowska-Curie Actions in 2023.